THE POTENTIAL AND LIMITATIONS OF INTRAVASCULAR OPTICAL COHERENCE TOMOGRAPHY

UDC 616.1–073.53
Received 4.10.2012

© **N.D. Gladkova,** D.Med.Sc., Professor, Head of Task Research Group of Optical Coherence Tomography, Scientific Research Institute of Applied and Fundamental Medicine[1]
E.V. Gubarkova, Junior Researcher, Scientific Research Institute of Applied and Fundamental Medicine[1]
E.G. Sharabrin, D.Med.Sc., Professor, Department of Radiology, the Faculty of Doctors Advanced Training; Director of Scientific Research Institute of Applied and Fundamental Medicine[1]
V.I. Stelmashok, PhD, Leading Researcher, Laboratory of Emergency and Interventional Cardiology[2];
A.E. Beimanov, Head of Angiography Department [3]

[1]Nizhny Novgorod State Medical Academy, Minin and Pozharsky Square, 10/1, Nizhny Novgorod, Russian Federation, 603005;
[2]Republic Scientific Practical Centre "Cardiology", R. Luxemburg St., 110, Minsk, Republic of Belarus, 220036;
[3]Emergency Hospital, Kizhevatova St., 58, Minsk, Republic of Belarus, 220024

The experience gained in the application of optical coherence tomography (OCT) for diagnosis and control of arterial sclerotic disease has been analyzed. The principles of OCT-image acquisition have been described, the advantages and disadvantages of intravascular OCT devices used in clinical practice have been assessed, and the safety and capabilities of intravascular OCT-procedure have been discussed. It has been demonstrated that intravascular OCT has great potential for understanding and treatment of arterial sclerotic disease. The capabilities of *in vivo* diagnosis of "vulnerable" atherosclerosis plaque and determination of calcium and macrophage content in atherosclerotic plaque, as well as features of coronarothrombosis have been addressed. Detailed attention has been given to the role of intravascular OCT in stenting follow-up. Possible ways of improvement of intravascular OCT and prospects of its further development have been considered.

Key words: intravascular optical coherence tomography; atherosclerotic plaque; stenting.

Optical coherence tomography (OCT) is an innovative medical diagnostic technique based on the principle of "vision in turbid media". It is used to obtain in real time high-contrast two- and three-dimensional images of internal structure of human body tissues at a depth of 1–2 mm with micron resolution. The technique is based on interferometry of infrared waves that have the highest penetration depth into biotissue [1]. The significant advantage of the technique is a capability to image internal organs using endoscopic probes [2–8].

It was presumed at the very beginning of OCT development that it may be a useful tool for imaging atherosclerotic process in arteries [9]. The method has a great potential in intravascular imaging as an alternative or a supplementary tool to intravascular ultrasound (IV US). In this overview we discuss the experience gained in the application of intravascular OCT (IV OCT) for diagnosis and control of arterial sclerotic disease. For illustrations we use intravascular OCT-images acquired on the OCT setup M2 (LightLab Imaging, Inc., USA) in the Republic Scientific Practical Centre "Cardiology" (Minsk, the Republic of Belarus) with reference to the materials from the web-site of Assomedica, the representing company of LightLab Imaging, Inc. in the Republic of Belarus [10].

The OCT principle

OCT is based on interference reception and measurement of backscattered broadband light in the infrared range [1]. The principle of OCT operation is similar to that of ultrasound and radar. But unlike the ultrasonic technique in which a signal caused by spatial distribution of acoustic impedance ("echo") is recorded, OCT receives light backscattered from optical inhomogeneities.

For contacts: Gladkova Nataliya Dorofeevna, tel. 8(831)465-41-13; e-mail: natalia.gladkova@gmail.com

In one of the simplest OCT modalities (time-domain OCT), radiation from the source is distributed in equal parts in the object and reference arm of an optical device — interferometer — by means of a beam splitter. Longitudinal (in depth) resolution element in images is determined by spectral width of the light source and can reach units of microns, which is one to two orders of magnitude higher than in conventional ultrasonic methods. Lateral resolution is determined by sharpness of focusing of broadband light by the optical system and can reach similar values. Images are acquired from a body *in vivo* in real time. OCT uses light at a wavelength in the 700–1300 nm range ("therapeutic transparency window"), where absorption is relatively low. Optical inhomogeneities are visualized with spatial resolution of 15–20 μm at a depth of 1–2 mm.

Recently, dramatic advance has been made in development of a new OCT modality based on spectral interferometry and referred to as frequency-domain OCT. As the great majority of results of clinical OCT applications were obtained using the conventional technique, in the present overview we will speak about OCT in terms of the "time-domain OCT".

Safety and feasibility of intravascular OCT procedure

By the early 2000s several clinical studies of IV OCT have been carried out that have demonstrated its superiority over IV US in imaging coronary arteries microstructure [11–15]. Red blood cells are known to cause multiple scattering and significant signal attenuation from arterial wall [13, 16, 17]. There arose a need to develop a stably operating catheter in which the examined area would be washed by a clear solution. Such a catheter was developed (Helios Occlusion Balloon Catheter, LightLab Imaging, Inc., Westford, Massachusetts, USA) (Fig. 1, *a*). The first study of its safety and IV OCT feasibility in clinical conditions was carried out on 76 patients with coronary heart disease in 8 centers in Japan in 2007 [18]. The OCT imaging system (ImageWire, Light Imaging Inc., Westford, Massachusetts) consists of a 0.006 inch fiber-optic core that rotates within a 0.016 inch transparent sheath. OCT imaging was performed during occlusion of the artery with a compliant balloon and continuous flushing. The OCT study was performed when the artery was occluded by an elastic balloon and the area of interest was continuously washed by Ringer's lactate solution. Vessel occlusion time was 48.3±13.5 seconds and occlusion-balloon pressure was 0.4±0.1 atmospheres. Flushing with lactated Ringer's solution was performed at a rate of 0.6±0.4 ml/s. No significant adverse events, including vessel dissection or fatal arrhythmia, were observed. Procedural success rates were 97.3% by OCT and 94.5% by IV US. The use of a motorized probe is limited by its diameter (0.016 inches), which hindered control of relatively long arterial segments (over 55 mm). The results of the investigations carried out by Yamaguchi T. et al. showed that the OCT catheter has advantages over IV US in imaging a narrow lumen. Minimum lumen diameter and area measurements were significantly correlated between OCT and IV US imaging

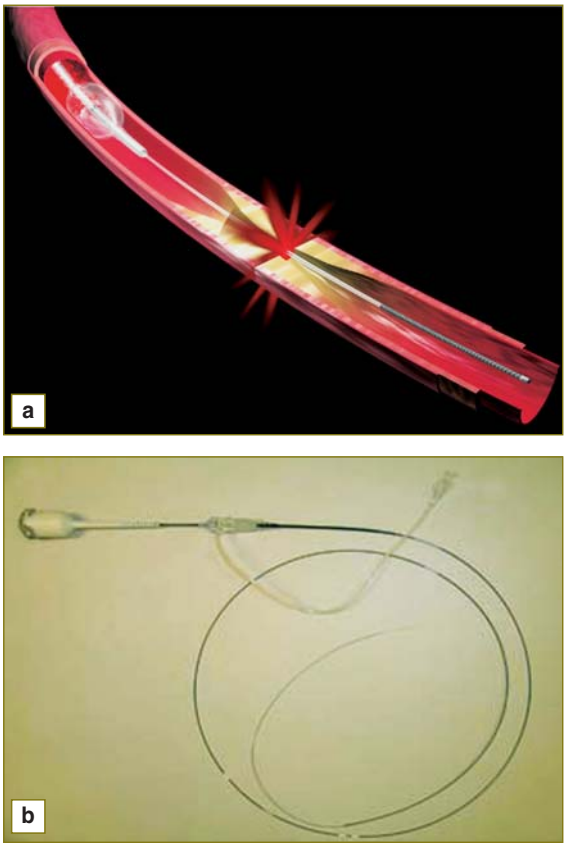

Fig. 1. Intravascular catheter: *a* — The OCT imaging system (ImageWire, Light Imaging Inc., Westford, Massachusetts) consists of a 0.006 inch fiber-optic core that rotates within a 0.016 inch transparent sheath [18]; *b* — new system C7 XR that does not need vascular occlusion at IV OCT-imaging; the catheter is connected through end *a* to the source of saline and contrast solution, and through end *b* to the device console, image acquisition takes just a few seconds [20]

(r=0.91, p<0.0001 and r=0.95, p < 0.0001, respectively) [18] (Fig. 2).

Later, F. Prati et al. [19] described a possibility of IV OCT imaging without proximal balloon occlusion of a vessel using iodixanol — an isomolar contrast substance injected from a conductor. This technique in combination with frequency domain OCT (C7 XR system that images 6-cm arteries within 3 s) requires injection of 4 ml of contrast substance per hour [20] (Fig. 1, *b*).

What does OCT image in arterial vessel and atherosclerotic plaque?

OCT enables imaging the structure of normal and atherosclerotic arteries. A normal arterial wall has a three-layer structure. The intima thickness in a normal vessel is usually 5–10 μm; it is outside the OCT resolution zone, hence, it is represented by a bright signal of internal elastic membrane. Media is represented by a low-intensity homogenous signal, and adventitia by a high-intensity signal [21].

The first OCT-images of atherosclerotic arteries were acquired by M.E. Brezinski et al. in the mid-90s in *ex vivo*

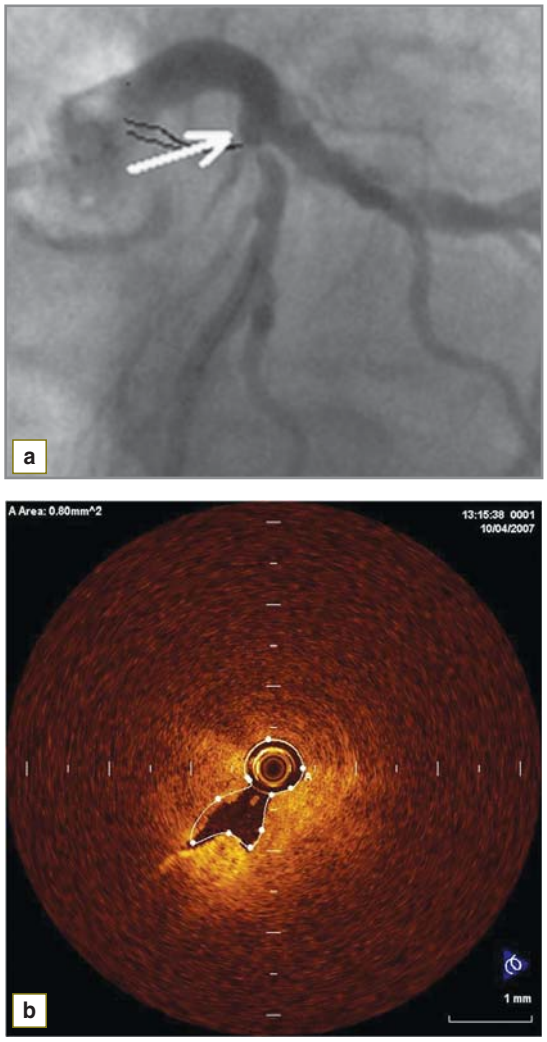

Fig. 2. Critical stenosis of anterior interventricular branch of left coronary artery: *a* — coronarography findings; the arrow indicates localization of stenosis zone at the border of segments 1 and 2 of anterior interventricular branch of left coronary artery; *b* — IV OCT; fissured lumen in the stenosis zone is visualized, lumen square is about 1 mm^2

sample of aorta. They demonstrated optical properties of fibroatheroma and calcified plaque [22]. In 2002 H. Yabushita et al. described OCT-features of different types of atherosclerotic plaques based on the correlation of OCT and histological images in a large autopsy series [23]. Fibrous tissue was characterized as a homogeneous area with intense signal, calcified tissue as a heterogeneous area with weak signal and well-defined boundaries, and lipid core tissue as a homogeneous area with weak signal and blurred boundaries. Sensitivity and specificity of the described features defined by the authors in *ex vivo* studies fell within the limits of 71–98% for fibrous plaque, 95–97% for atherosclerotic plaque with calcification, and 90–94% for lipid rich plaque (κ criterion was 0.83–0.84). Later, I.K. Jang et al. confirmed those data and showed that the same criteria are applicable to images obtained *in vivo* [13]. It was also found [24] that macrophage foam cells can be detected and quantified with high accuracy. Further those observations were confirmed by other researchers and laid the basis for developing a visual characteristic standard of OCT-images [17, 21, 25].

IV OCT has a fairly wide potential in atherosclerosis diagnosis.

1. *In vivo diagnosis of "vulnerable" plaque*. A thin fibrous cap is a well known feature of atherosclerotic plaque that results in its rupture. The criteria of unstable "vulnerable" plaque susceptible to rupture were set forth by R. Virmani et al. [26, 27]: mean plaque size 2–3 mm in diameter; the presence of a lipid core and plaque hemorrhage (when the core occupies over 40% of plaque volume); fibrous cap thickness less than 65 μm; a small amount of type I collagen and predominance of type III collagen in the cap; angiogenesis of intima and high degree inflammation inside the cap. High resolution of OCT allows *in vivo* identification of a thin fibrous cap less than 65 μm.

2. *Imaging of macrophages*. Macrophages are inherent in atherosclerotic plaques and play an important role in their origin, evolution, and rupture. OCT is able to detect macrophages and assess their number. Immunoperoxidase staining CD 68 is a standard of determining the number of macrophages in such studies [24].

3. *Imaging of coronarothrombosis features.* T. Kume et al. were the first to assess coronary arterial plaque by OCT [25]. Red thrombi are identified as protrusions in arterial cavity with high-intensity signal, whose shadow completely shields the signal. White thrombi are imaged as formations with intense signal that are projected onto the vessel wall and attenuate the signal in this area but to a lesser degree than the red thrombi.

4. *Stents follow-up* [11, 28, 29]. IV US cannot accurately image neointima tissue, if it consists of several cell layers only. OCT provides more accurate information about hyperplasia rate of neointima on stent struts [15, 29–31]. OCT is a potentially promising technique when working with stents, as well as in early diagnosis of complications related to this procedure, and long-term follow-up of patients.

5. *Separate assessment of plaque elements*. OCT enables differentiating between smooth muscle cells and collagen fibers. Collagen polarization properties allow using polarization-sensitive OCT [32].

Let us consider in detail the mentioned IV OCT capabilities.

Diagnosis of unstable ("vulnerable") plaque. Today OCT is the best tool for detecting an unstable plaque. This assertion is based on the results of a number of studies. The work of T. Kubo et al. [33] comparing the capabilities of IV OCT, IV US and angioscopy in patients with acute myocardial infarction showed that OCT is a leader in detecting plaque rupture (73% versus 40 and 43%, respectively; p=0.021), erosion (23% versus 0 and 3%; p=0.003), and thrombus (100% versus 33 and 100%; p<0.001); κ criterion was 0.61–0.83. High resolution of OCT permits *in vivo* identification of thin fibrous cap (<65 μm) (Fig. 3).

T. Kume et al. [34] studied OCT reliability in determining fibrous cap thickness. The assessment of 35 plaques *ex vivo* in 38 cases showed high correlation of fibrous cap thickness in histology and OCT-images (r=0.9; p<0.001). T. Sawada et al. [35] compared the capabilities of OCT and

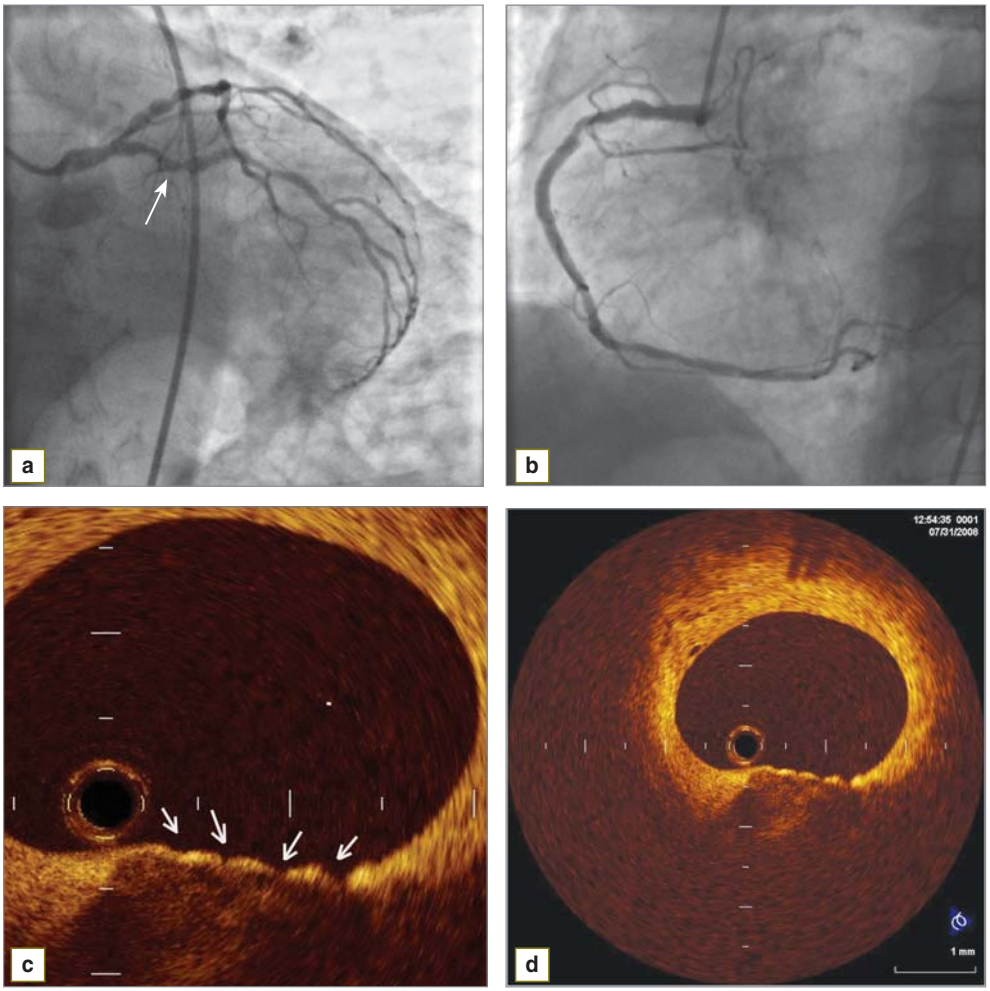

Fig. 3. Unstable atherosclerotic plaque: *a, b* — coronarography findings: multifocal lesions of coronary arteries, nonuniform staining was detected proximally to stenosis in circumflex branch (arrow) that was suspicious for the presence of recanalized thrombus in this zone; *c*, *d* — IV OCT is performed proximally to stenosis in circumflex branch (arrow in Fig. *a*); detected: absence of recanalized thrombosis in the studied zone; "incidental" finding: erosion of atherosclerotic plaque cap (arrows indicate erosion zones in Fig. *c*) indicating unstable atherosclerotic plaque

IV US for detecting thin cap fibroatheroma. OCT potential turned out to be clearly higher: 77.8% versus 45.9%. T. Kubo et al. [36] assessed the relationship between plaque color at angioscopy and fibrous cap thickness in OCT-image. Negative correlation between yellow color intensity and fibrous cap thickness was found ($p<0.0001$). M. Kashiwagi et al. [37] compared the capabilities of OCT and computer tomography in assessment of the thickness of fibroatheroma cap at acute coronary syndrome and showed the superiority of OCT. I.K. Jang et al. [17] analyzed OCT-images of 57 patients, including patients with stable angina pectoris, unstable angina pectoris, and acute myocardial infarction. In the case of acute myocardial infarction, compared to the other groups, plaque coverage was thinner and contained more lipids (72% versus 50 and 20%, respectively; $p=0.012$). K. Fujii et al. [38] carried out prospective analysis of the three principal coronary arteries aiming at assessing the rate and predictive value of detecting plaques with a thin cap in patients with acute myocardial infarction and stable angina pectoris. Thin-walled plaques were more frequent in patients with acute myocardial infarction than in those with stable angina pectoris (69 versus 10%; $p<0.001$). Multivariate analysis of the whole group showed that predictive value of this feature (in terms of Odds Ratio — OR) is sufficient for acute myocardial infarction only (OR=4.12; 95% CI=2.35–9.87; $p=0.02$).

It is possible to measure fibrous cap thickness using OCT, but accuracy is not guaranteed. The interface between fibrous cap and lipid core, that is so well-defined histologically, is not always determined accurately by OCT if lipid accumulation is small. OCT-images are reliable for identification of fibroatheroma thin cap in large-size plaques only [33, 35].

Coronary calcinosis diagnosis. Calcinosis of coronary arteries is an important atherosclerosis marker [39–41]. Noninvasive calcium measurement is generally performed by means of computer tomography [42, 43] or IV US. OCT visualizes calcium as an area with a low signal and well-defined boundaries. Calcium deposits can be detected by

OCT with high sensitivity (96%) and specificity (97%) [23]. The principal advantage of OCT over the other calcium imaging techniques is the capability of obtaining a three-dimensional image of calcium area that cannot be made by IV US due to low penetration of ultrasound into calcium formations [40]. Computer tomography can assess calcium volume indirectly [44], but low resolution of the technique (about 1 mm) does not give an accurate picture of plaque structure. OCT provides the highest resolution with better penetration into calcium deposits as compared to other methods. The presence and degree of surface calcification may have a significant impact on percutaneous coronary intervention success, as it may cause vascular dilatation and thrombosis under the stent [45]. Therefore, OCT can be employed for collecting data on the amount of calcium and its location relative to the vascular lumen, which is a useful complementary tool to rotational atherectomy and ballooning [46].

Another important application is automatic OCT assessment of calcium volume, as well as determination of the depth and degree of coronary vessel calcification in percutaneous coronary intervention. Automatic calcium detection is of great importance for comprehensive analysis, and can indicate optimal areas for stent implanting [47, 48].

Detection of macrophages (foam cells). Foam cells — cholesterol-filled macrophages — are detected both at an early stage of atherosclerosis, and later, in lipid-rich plaques [49]. High density of macrophages correlates with high risk of plaque rupture and is associated with acute coronary events [50]. Researches carried out in 2000s showed that OCT is able to identify macrophages [24, 51, 52]. Foam cells have a refraction index different from that of extracellular environment. OCT images macrophages as spots with a high intensity signal. G.J. Tearney et al. [24] hypothesized that macrophages contribute to high inhomogeneity of a signal and to determine the amount of macrophages they used normalized standard deviation of the intensity of a randomly chosen signal within the window in a fibrous cap. In further clinical research they determined the relationship between macrophage distribution and clinical manifestations of coronary disease [52]. IV OCT was used to study plaques that were or were not the cause of coronary disease in patients with stable angina pectoris, unstable angina pectoris, and acute myocardial infarction. The density of macrophages was estimated quantitatively and correlated with clinical manifestations. High density of macrophages was revealed in patients with unstable angina pectoris both in fibrous and lipid-rich plaques ($p=0.025$ and $p=0.002$, respectively). Macrophage density in plaques that were or were not related to clinical manifestations of coronary disease correlated statistically significantly ($r=0.66$; $y=0.88$; $x=0.43$; $p=0.01$) in each patient. In the area of plaque rupture, the macrophages density was statistically significantly higher than in the area without rupture (6.95±1.60%; 5.29±1.17%; $p=0.002$). The areas of surface macrophage infiltration predicted unstable clinical manifestations better than those with deep infiltration. The results showed that macrophage density is closely related to the severity of clinical symptoms. Reliable means of macrophage foci detection before coronary events can help to predict rupture and provide effective prevention.

B.D. MacNeill et al. [52] selected a segment of fibrous cap to be treated automatically using a bimodal histogram. There is an opinion [53] that this technique does not reflect true density of macrophages within cap, as there may be various reasons for increased signal (in particular, any tissue and cell boundaries). The authors of [53] believe that only OCT modalities with ultra high resolution (1–5 μm) can provide reliable imaging of macrophages.

Coronarothrombosis diagnosis. It has been shown in a number of works that OCT can detect intracoronal thrombi that are imaged as masses protruding in vascular lumen. Red thrombi consist mainly of red blood cells and are characterized by appreciable signal attenuation, whereas white thrombi are generally composed of white blood cells and platelets and are characterized by low signal attenuation.

The characteristics of coronarothrombosis in OCT-images were studied by T. Kume et al. [25] in 108 segments of coronary arteries ex vivo in from 40 cases. Red thrombi were identified as protrusions into arterial cavity with high-intensity signal, whose shadow completely shields the signal. White thrombi are visualized as masses with intense signal projected onto a vascular wall and attenuate the signal to this area, but to a lesser degree than the red thrombi. No difference in the intensity of OCT-signal from red and white thrombi was revealed (130±18 versus 145±34 U, $p=0.12$). Nevertheless, 1/2 of the width of signal attenuation of red and white thrombi was significantly different (324±50 versus 183±42 μm; $p<0.0001$). The threshold value of 250 μm of 1/2 width of signal attenuation can be a differential sign of white thrombus with 90% sensitivity and 88% specificity [25, 47, 54].

Other authors in their studies of acute coronary syndrome have also demonstrated OCT potential in thrombus detection [33]. However, it is difficult, especially in stenting, to distinguish thrombi from other tissues abnormally appearing in vascular lumen. Residual amount of blood in coronary artery as a result of inadequate substitution by clear solution, fibrin or intimal flaps can mimic thrombi. E.A. Mehanna et al. [55] suggested using a more general term “abnormal tissues inside lumen” (ATIL) for description of these structures until more objective evidence is obtained. ATIL is an intraluminal material connected with a vascular wall and protruding into lumen, thereby forming an irregular surface and “shadowing” with significant signal attenuation (Fig. 4). ATILs were divided into 4 groups according to stent strut coverage, presence of neointima, and restenosis location within a stent. This approach helps interpreting difficult clinical cases.

Study of coronary stents. OCT is a robust tool to study stents. There is every reason to believe that in the near future OCT will become a technique for *in vivo* assessment of stent condition and its synergy with vessels. According to L.J. Diaz-Sandoval et al. [11], E. Regar et al. [28] and Y. Suzuki et al. [29], OCT can be helpful in percutaneous coronary interventions in the process of stent implantation. E. Regar et al. [28] demonstrated successful use of

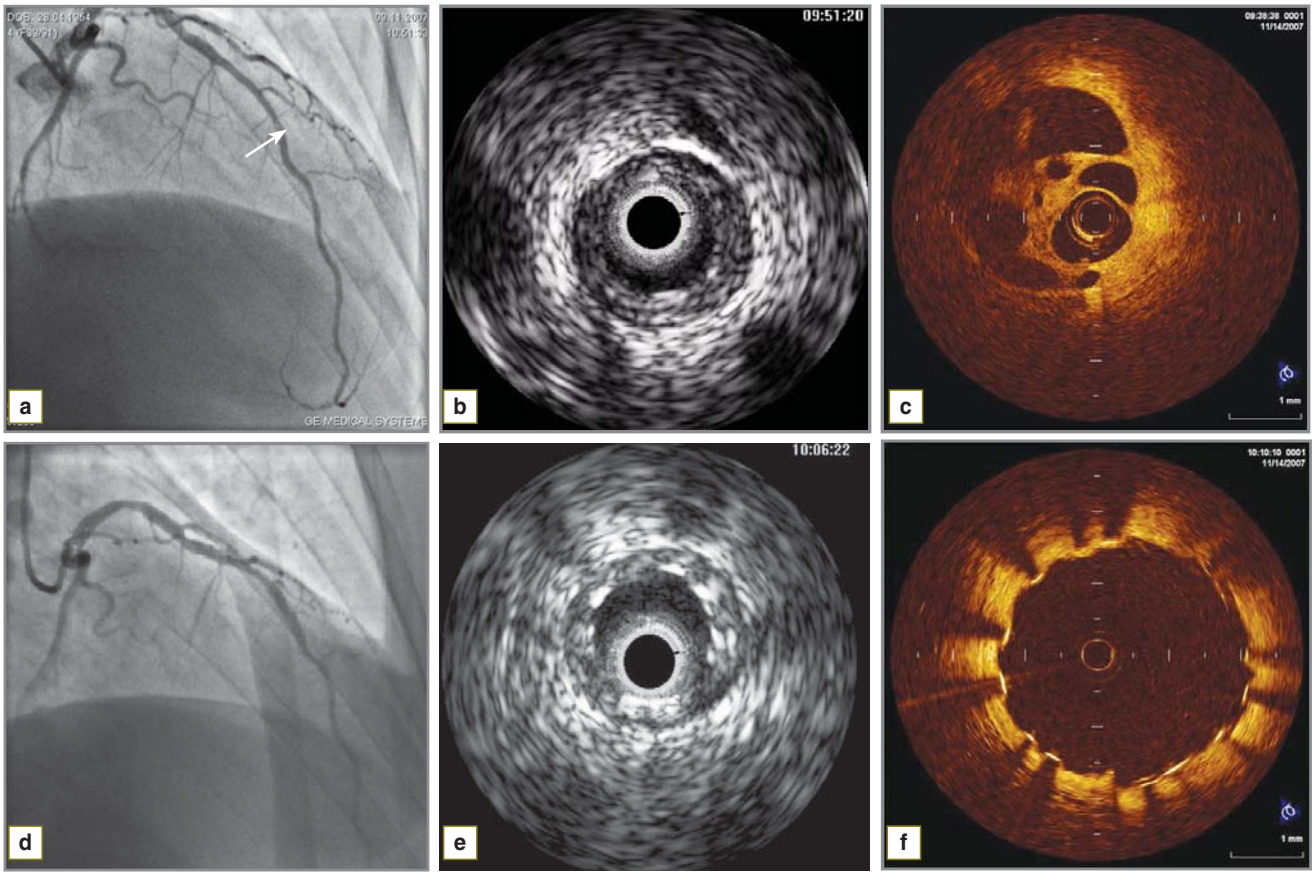

Fig. 4. Recanalized thrombus in segment 2 of anterior interventricular branch of left coronary artery: *a* — angiography findings: the arrow indicates transilluminated zone; *b* — IV US findings: concentric plaque is visualized in arterial region with angiographically detected transilluminated zone; *c* — IV OCT findings: honey-comb structure — recanalized thrombus is visualized in arterial region with angiographically detected transilluminated zone; *d, e, f* — condition after stent implantation in the zone of recanalized thrombus (full adhesion of stent struts to vascular wall is verified by IV OCT, Fig. *f*)

OCT for choosing in real time an optimal place for stent implantation. Y. Suzuki et al. [29] showed that OCT may be used to optimize angles between struts after opening of drug-eluting stents that are known to to be able to restrict neointima growth significantly.

IV US cannot visualize neointima accurately if it consists of several cell layers. OCT provides more reliable information about neointima coverage of struts of a drug-eluting stent and permits determining layer width [15, 31]. In addition, sirolimus-eluting stents tend to develop late thrombosis that frequently results in various complications, including acute myocardial infarction. OCT can inform of the process of neointima formation on sirolimus-eluting stents [31, 56]. This information can be helpful for timely use of anti-platelet or anti-coagulation therapy in such patients and for long-term monitoring of patients.

IV OCT provides *in vivo* detailed analysis of stent strut condition [57]. The basic parameters of stent implantation, such as vascular diameter and strut malposition are better evaluated by OCT than IV US [58] (Fig. 5). OCT enables detailed visualization of tissue stent coverage and its further analysis [59].

In several recently published researches, OCT was used to assess drug-eluting stents [60–62]. The technique of OCT-imaging and analysis to assess stents was proposed by G. Guagliumi et al. [63, 64]. It is important to receive information on stent full length. A simple way to estimate total length of a stent is to observe high echo signal generated by bare-metal stent struts, even through whole (undiluted) blood. This property can be used in clinical conditions to position catheter distally to the region of interest to cover stent's full length. The catheter may be removed until stent struts disappear in the image, which indicates that the distal stent edge has been passed.

High resolution of OCT has apparent advantage over IV US in case of long-term stent follow-up, especially in quantitative assessment of neointima hyperplasia [59, 65].

The majority of stents (bare-metal or drug-eluting stents) are made of metals and their alloys. Light scatters completely (mirror reflection) on stent struts surface forming a hypersignal usually called "florescence". As light cannot pass through metal, a shadow is formed behind the "florescence". Although this phenomenon also occurs in IV US, it is more pronounced in OCT because of its better resolution. An operator should be aware of the phenomenon to avoid misinterpretation of images. Both features ("florescence" and shadow) are helpful in identifying separate struts, which is necessary for qualitative and quantitative analysis of OCT-images (Fig. 6).

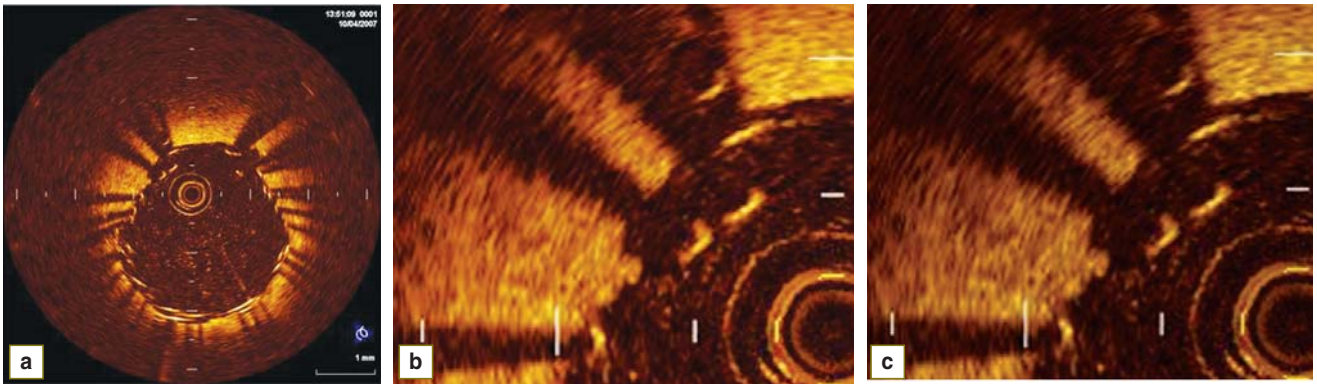

Fig. 5. Poorly outspread: *a, b, c* — IV OCT findings with different degree of image magnification: incomplete adhesion at the junction of struts of the stents implanted both to each other, and to a vascular wall, indicating incomplete stent apposition in this vascular area (incomplete stent apposition is at 11 o`clock, and at 1–2 o`clock)

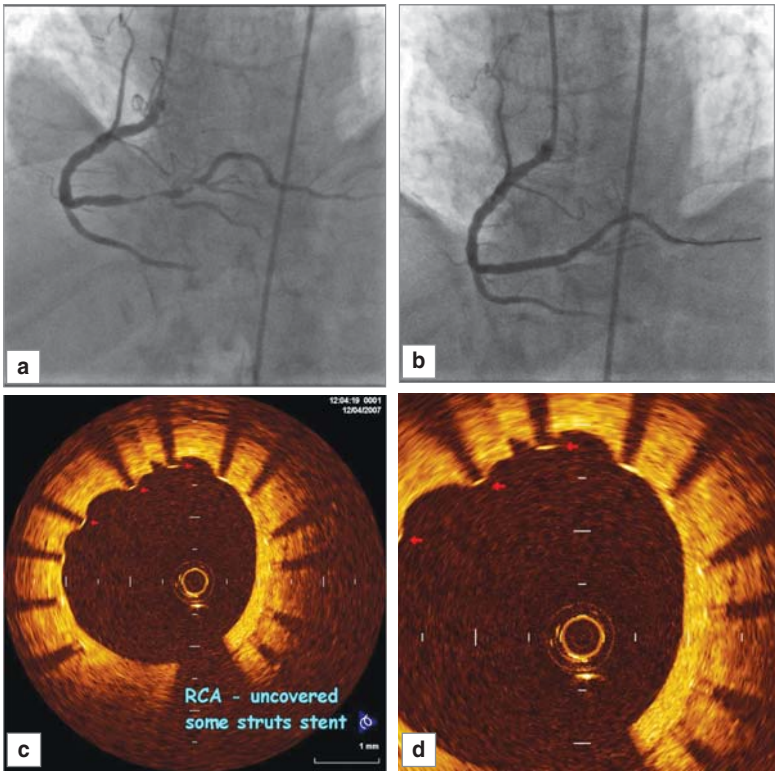

Fig. 6. Incomplete endothelization of bare-metal stent Medtronic S 670 struts 1 year after implantation: *a, b* — coronarography findings before stenting and 1 ear after; *c, d* — IV OCT: incomplete endothelization of struts of implanted bare-metal stent 1 year after implantation is revealed (stent struts not covered by endothelium are localized at 9–12 o`clock — red arrows)

Bioresorbable polymer stents (in contrast to bare-metal stents) transmit light, facilitating formation of three-dimensional OCT-images. Struts of such stents are visualized as "boxes" with well-defined boundaries. This allows reliable imaging of everolimus-eluting bioresorbable stents apposition, as well as observe their gradual degradation until total polymer disappearance and neointima formation [66].

OCT records various failures in stent implantation: incomplete stent apposition with strut malposition; dissection of vascular wall proximally or distally to the implanted stent; dissection in the stented segment; tissue protrusion between stent struts (Fig. 7).

Neointimal thickness in long-term follow-up period after stent implantation can be assessed by OCT to high accuracy comparable with histology findings [67]. At moderate hyperplasia neointima is clearly seen only in OCT-images. Usually it occurs when bioresorbable stents with potent agents are used [60, 65]. In pilot studies [68] on 250 stented segments with neointima undetectable by IV US, it was identified by OCT in 97% of cases. These findings confirm the necessity of using high resolution techniques for adequate study of bioresorbable stents. The highest risk of adverse consequences due to failure of stent strut opening is caused stent thrombosis development [69] (Fig. 8). Large areas of incomplete stent apposition are also known to correlate with the risk of stent thrombosis [70]. Hence, assessment of the efficiency of stent opening after implantation is of primary importance. In contrast to IV US that demonstrates only cross section, high-resolution OCT provides detailed *in vivo* information about every element of stent struts [71–74].

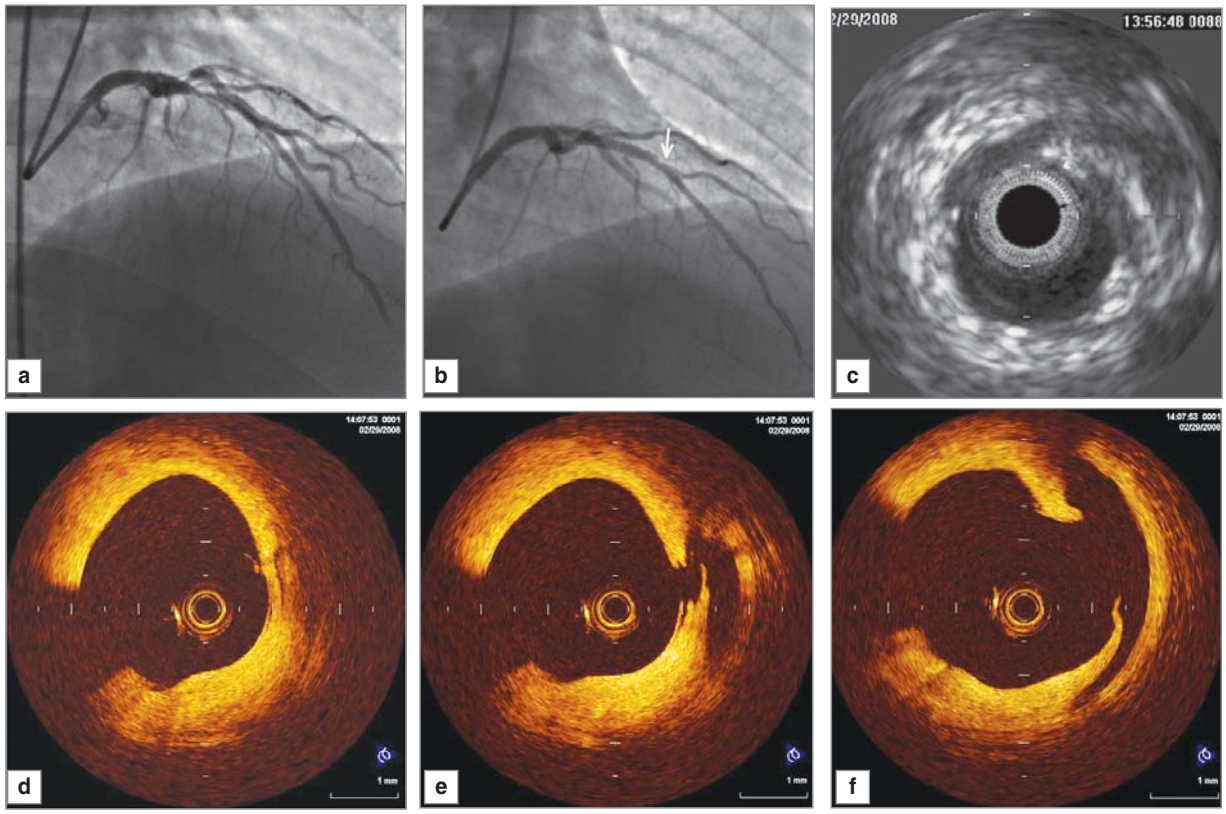

Fig. 7. Dissection after stent implantation: *a* — coronarography findings before stenting, the presence of critical stenosis in segment 2 of anterior interventricular branch of left coronary artery is revealed; *b* — coronarography findings after stenting, the presence of intimal dissection distally to implanted stent zone is revealed (white arrow indicates dissection zone); *c* — IV US findings (intimal dissection zone at 10–12 o`clock); *d* — IV OCT, dissection onset (linear dissection zone in intimal depth at 3 o`clock, with no clearly visualized communication with vascular lumen); *e* — IV OCT, intimal rupture at 3 o`clock with clearly visualized communication of vascular lumen with formed subintimal space; *f* — IV OCT, maximally evident zone of intimal rupture at 3 o`clock with clearly visualized communication of vascular lumen with formed subintimal spac

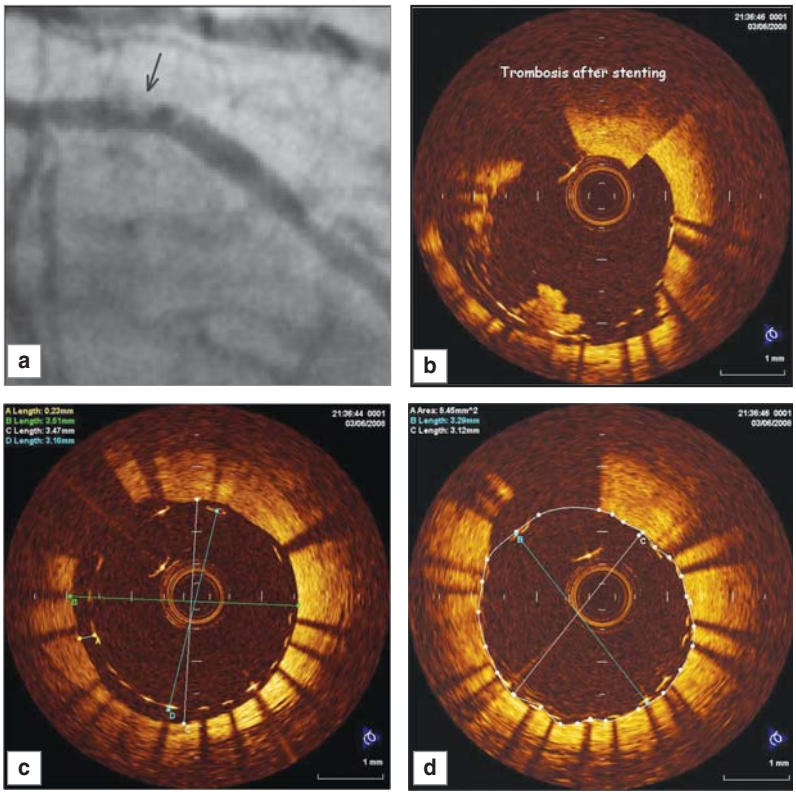

Fig. 8. Acute thrombosis 40 min after percutaneous coronary intervention (the cause of acute thrombosis — incomplete stent apposition): *a* — coronarography findings 40 min after stenting; visualized are areas of inhomogenous transillumination in anterior interventricular branch of left coronary artery (black arrow); *b* — IV OCT findings, presence of parietal non-occlusive thrombus at 7 o`clock and areas of incomplete adhesion of stent struts to vascular wall at 5–8 o`clock; *c* — IV OCT findings, poor adhesion of stent struts to vascular wall at 5–12 o`clock indicating incomplete spread of the stent in this vascular region; *d* — IV OCT, adequate adhesion of stent struts to vascular wall in the zones demonstrated in Fig. *b*, *c*, after repeated postdilatation by high-pressure coronary balloon catheter

Advantages and limitations of intravascular OCT

The IV OCT advantages may be assessed by the following aspects [32]:

Merits of the technique — safety, high spatial resolution, high speed of imaging.

Merits of the device — low cost, mobility, use of endoscopic probes, imaging of vascular lumen; compact, inexpensive OCT catheter directly images tissue structure without converter.

Unique clinical capabilities — safe multiple repeated application; high-speed operation and acquisition of information in real time make OCT helpful for intraoperative use; ability to visualize calcifications in plaques, image hyperplastic neointima, monitor stent behavior and predict atherosclerotic plaque behavior based on its morphological features.

Comparative studies of IV OCT and IV US showed that all plaques identified by IV US were recognized in OCT-images. It is worthy of notice that neointimal hyperplasia and areas with low echogenicity were better identified by IV OCT. OCT is superior in detecting plaque composition. It was found that some complications in stent implanting undetected by IV US were successfully identified by OCT. As compared with IV US, OCT has better resolution (10–15 μm versus 100 μm), whereas IV US can visualize through blood and penetrate deeper in tissue (1 cm versus 2–3 mm). OCT is effective in stenting procedures, since it easily identifies stent position.

With all advantages of IV OCT, it has limitations. One of OCT limitations is its small penetration depth; visualization is limited to 2–3 mm, which significantly worsens the quality of imaging the arteries with necrosis.

Intracoronary OCT imaging is in not widely used in clinical practice as infrared radiation does not penetrate through blood. Therefore, unlike IV US, IV OCT requires transillumination or washing out of blood from vascular lumen [23, 25, 75, 76]. This limitation is eliminated by creating special accessories used both in noncommercial time-domain OCT modality developed by I.K. Jang et al. [13], and in automated systems approved by FDA and now manufactured by LightLab Imaging, Inc. (USA) and St. Jude Medical (USA).

The main limitations of IV OCT are considered to be failure to remodel the entire arterial wall thickness due to strong signal attenuation on red blood cells, and a possibility of myocardial ischemia development due to the necessity of continuous vascular occlusion by balloon catheter aimed at improving vascular wall imaging. The use of new technologies (including frequency-domain OCT) permits overcoming some of these technical difficulties and contributes to more extensive use of the method as a reliable diagnostic and therapeutic tool in cardiology [77].

Possible ways of improving intravascular OCT

The technique can be improved in several directions.

Improvement of tissue characteristics by using advanced OCT modalities. Fibrous cap and lipid core contrast may be enhanced using polarization-sensitive OCT that measures tissue birefringence [78, 79]. Well organized collagen fibers and smooth-muscle cells are known to be more birefringent than disorganized plaque constituents, such as lipid tissue. However, birefringence can be accurately measured only at a relatively deep depth (e.g., 200 μm) that is much deeper than the thickness of a thin fibrous cap (65 μm) in vulnerable plaques.

Doppler OCT can become a handy tool to assess tissue perfusion [80–82].

Qualitative assessment of OCT images is useful for objective diagnosis and making clinical decisions for treatment. An OCT-signal is known to be determined by scattering and attenuation coefficients in tissue. These coefficients were first measured on arteries *ex vivo* [83, 84]. However, plaques are generally multilayered, which complicates accurate correlation of histological data and OCT information. C. Xu et al. suggested measuring cross-section of a dissected artery, in which every plaque component can be measured and easily identified histologically [85]. OCT-images on the plaque showed that a lipid area in the upper layer demonstrates an intense signal, and signal attenuation is observed only in deeper layers. Backscattering and attenuation coefficients were determined for all types of plaques: for calcified tissue (μ_1=4.9±1.5 mm^{-1}; μ_2=5.7±1.4 mm^{-1}), fibrous tissue (μ_1=8.4±6.4 mm^{-1}; μ_2=6.4±1.2 mm^{-1}), and lipid tissue (μ_1=28.1±5.9 mm^{-1}; μ_2=13.7±4.5 mm^{-1}). Attenuation coefficient was also measured for a rotational OCT-image: normal vascular wall and intimal thickening — 2–5 mm^{-1}; necrotic nucleus >10 mm^{-1}; macrophage infiltration >12 mm^{-1} [86]. Quantitative analysis enabled a new approach to interpreting OCT-images.

Development of frequency-domain (spectral) OCT. With the advent of frequency-domain equipment, OCT has progressed from point high-resolution images to comprehensive microscopic imaging over three-dimensional volumes that are comparable to the dimensions of internal organs lumen. This demanded development of new lasers, improved spectrometers, minimum invasive catheters and endoscopes, as well as elaboration of a new strategy of optical signal processing. Recent investigations of frequency-domain OCT in cardiovascular, ophthalmic, and gastrointestinal clinical areas have opened up new opportunities for diagnostic screening of large areas of tissues, inaccessible before. New appropriate catheters have been developed that provide minimally invasive access to the main coronary arteries. As was mentioned above, the major problem of IV OCT is that blood is almost nontransparent to probe radiation and should be substituted by a clear saline solution for a short period of the study. Such a substitution can take place without ischemia risk within a few seconds only. Clinical studies of OCT demonstrated fine quality images, although the earlier-generation technologies allowed acquiring several frames per second, which made it possible to visualize discretely only a small part of coronary arteries. The recent advance — frequency-domain OCT development — has overcome this limitation, increased imaging rate up to over 100 frames per second. This increase enables visualizing long segments of coronary artery after a short (units of seconds) iodixanol

injection into a guiding catheter, and therefore, 3D imaging of the whole coronarothrombosis section [7, 87]. The capability to visualize a large part of artery is of critical importance for performing angioplasty and stenting.

It is quite possible that signal processing will be an important field of technical development of the next-generation OCT-systems. Currently, OCT systems can transmit data at a speed of 1 Gb/s. New algorithms are demanded for image interpretation for automatic diagnosis or for separating data to be interpreted by man. Future work is likely to result in integration of techniques aimed at enhancement of contrast and molecular specificity of the frequency-domain OCT. Many methods developed for the time-domain OCT, including Doppler OCT [88, 89], polarization-sensitive OCT [90–92], and biochemical approaches [93–95] can be transferred directly to the new frequency-domain platform. It is worthy of notice that many OCT techniques have already been realized in the frequency-domain: Doppler [96–99] and polarization-sensitive [97, 100, 101] OCT. Currently, over ten companies are ready to come into the market with OCT-systems of the new generation.

Conclusion. Intravascular optical coherence tomography has a huge potential for understanding and management of atherosclerotic heart disease. Up to date there is no technique, except OCT, that would be as useful in "vulnerable" plaque identification, assessing of calcium amount, and monitoring of stenting. The OCT technique is constantly developing and has good prospects for further expansion.

The study was carried out under the terms of the Federal Target Program of the Ministry of Education and Science of the Russian Federation "Scientific and academic and teaching staff of innovative Russia" 2009-2013, Agreement No.8145; Russian Foundation for Basic Research grant No.10-02-01175 and the grant of the Government of the Russian Federation (Contract No.1.G34.31.0017).

References

1. *Rukovodstvo po opticheskoy kogerentnoy tomografii* [Handbook of optical coherence tomography]. Pod red. Gladkovoy N.D., Shakhovoy N.M., Sergeeva A.M. [N.D. Gladkova, N.M. Shakhova, A.M. Sergeev (editors)]. Moscow: Fizmatlit; 2007; 296 p.

2. Rollins A.M., Ung-arunyawee R., Chak A., Wong R.C.K., Kobayashi K., Sivak M.V., Izatt J.A. Real-time in vivo imaging of human gastrointestinal ultrastructure by use of endoscopic optical coherence tomography with a novel efficient interferometer design. *Opt Lett* 1999; 24 (19): 1358–1360.

3. Tearney G.J., Boppart S.A., Bouma B.E., Brezinski M.E., Weissman N. J., Southern J.F., Fujimoto J.G. Scanning single-mode fiber optic catheter-endoscope for optical coherence tomography: erratum. *Opt Lett* 1996; 21(12): 912.

4. Tearney G.J., Brezinski M.E., Bouma B.E., Boppart S.A., Pitris C., Southern J.F., et al. In vivo endoscopic optical biopsy with optical coherence tomography. *Science* 1997; 276: 2037–2039.

5. Xi J., Huo L., Wu Y., Cobb M.J., Hwang J.H., Li X. High-resolution OCT balloon imaging catheter with astigmatism correction. *Opt Lett* 2009; 34(13): 1943–1945.

6. Yun S.H., Tearney G.J., Vakoc B.J., Shishkov M., Yelin R., Oh W.Y., et al. Comprehensive volumetric optical microscopy in vivo. *Nat Med* 2006; 12: 1429–1433.

7. Sergeev A.M., Gelikonov V.M., Gelikonov G.V., Feldchtein F.I., Kuranov R.V., Gladkova N.D., et al. In vivo endoscopic OCT imaging of precancer and cancer states of human mucosa. *Optics Express* 1997; 1(13): 432–440.

8. Jäckle S., Gladkova N., Feldchtein F., Terentieva A., Brand B., Gelikonov G., Gelikonov V., Sergeev A., Fritscher-Ravens A., Freund J., Seitz U., Soehendra S., Schrödern N. In vivo endoscopic optical coherence tomography of the human gastrointestinal tract-toward optical biopsy. *Endoscopy* 2000; 32(10): 743–749.

9. Huang D., Swanson E.A., Lin C.P., Schuman J.S., Stinson W.G., Chang W., et al. Optical coherence tomography. *Science* 1991; 254; 1178–1181.

10. http://www.assomedica.by/Presentations.

11. Diaz-Sandoval L.J., Bouma B.E., Tearney G.J., Jang I.K. Optical coherence tomography as a tool for percutaneous coronary interventions. *Catheter Cardiovasc Interv* 2005; 65: 492–496.

12. Grube E., Gerckens U., Buellesfeld L., Fitzgerald P.J. Images in cardiovascular medicine. Intracoronary imaging with optical coherence tomography: a new high-resolution technology providing striking visualization in the coronary artery. *Circulation* 2002 Oct 29; 106(18): 2409–2410.

13. Jang I.K., Bouma B.E., Kang D.H., Park S.J., Park S.W., Seung K.B., et al. Visualization of coronary atherosclerotic plaques in patients using optical coherence tomography: comparison with intravascular ultrasound. *Journal of the American College of Cardiology* 2002 Feb 20; 39(4): 604–609.

14. Jang I.K., Tearney G., Bouma B. Visualization of tissue prolapse between coronary stent struts by optical coherence tomography-comparison with intravascular ultrasound. *Circulation* 2001 Nov 27; 104(22): 2754.

15. Kume T., Akasaka T., Kawamoto T., Watanabe N., Toyota E., Sukmawan R., et al. Visualization of neointima formation by optical coherence tomography. *Int Heart J* 2005 Nov; 46 (6): 1133–1136.

16. Brezinski M., Saunders K., Jesser C., Li X., Fujimoto J. Index matching to improve OCT imaging through blood. *Circulation* 2001 April 17; 103(15): 1999–2003.

17. Jang I.K., Tearney G.J., MacNeill B.D., Takano M., Moselewski F., Iftima N., et al. In vivo characterization of coronary atherosclerotic plaque by use of optical coherence tomography. *Circulation* 2005; 111: 1551–1555.

18. Yamaguchi T., Terashima M., Akasaka T., Hayashi T., Mizuno K., Muramatsu T., et al. Safety and feasibility of an intravascular optical coherence tomography image wire system in the clinical setting. *Am J Cardiol* 2008; 101: 562–567.

19. Prati F., Cera M., Ramazzotti V., Imola F., Giudice R., Albertucci M. Safety and feasibility of a new non-occlusive technique for facilitated intracoronary optical coherence tomography (OCT) acquisition in various clinical and anatomical scenarios. *EuroIntervention* 2007; 3: 365–370.

20. Herrero-Garibi J., Cruz-Gonzalez I., Parejo-Diaz P., Jangc I.-K. Optical coherence tomography: its value in intravascular diagnosis today. *Rev Esp Cardiol* 2010; 63(8): 951–962.

21. Rieber J., Meissner O., Babaryka G., Reim S., Oswald M., Koenig A., et al. Diagnostic accuracy of optical coherence tomography and intravascular ultrasound for the detection and characterization of atherosclerotic plaque composition in ex vivo coronary specimens: a comparison with histology. *Coron Artery Dis* 2006; 17: 425–430.

22. Brezinski M.E., Tearney G.J., Bouma B.E., Izatt J.A., Hee M.R., Swanson E.A., et al. Optical coherence tomography for optical biopsy: properties and demonstration of vascular pathology. *Circulation* 1996; 93: 1206–1213.

23. Yabushita H., Bouma B.E., Houser S.L., Aretz H.T., Jang I.K., Schlendorf K.H., et al. Characterization of human atherosclerosis by optical coherence tomography. *Circulation* 2002 Sep 24; 106(13): 1640–1245.

24. Tearney G.J., Yabushita H., Houser S.L., Aretz H.T., Jang I.K., Schlendorf K.H., et al. Quantification of macrophage content in atherosclerotic plaques by optical coherence tomography. *Circulation* 2003; 107: 113–119.

25. Kume T., Akasaka T., Kawamoto T., Watanabe N., Toyota E., Neishi Y., et al. Assessment of coronary arterial plaque by optical coherence tomography. *Am J Cardiol* 2006 Feb; 97: 1172–1175.

26. Virmani R., Kolodgie P.D., Burke A.P., Farb A., Schwartz S.M. Lessons from sudden coronary death: a comprehensive morphological classification scheme for atherosclerotic lesions. *Arterioscler Thromb Vasc Biol* 2000; 20: 1262–1275.

27. Virmani R., Burke A.P., Farb A., Kolodgie P.D. Pathology of unstable plaque. *Prog Cardiovasc Dis* 2002; 44: 349–356.

28. Regar E., Schaar J., Serruys P.W. Images in cardiology. Acute recoil in sirolimus eluting stent: real time, in vivo assessment with optical coherence tomography. *Heart* 2006 Jan; 92(1): 123.

29. Suzuki Y., Ikeno F., Yeung A.C. Drug-eluting stent strut distribution: a comparison between Cypher and Taxus by optical coherence tomography. *J Invasive Cardiol* 2006; 18: 111–114.

30. Ito S., Itoh M., Suzuki T. Intracoronary imaging with optical coherence tomography after cutting balloon angioplasty for in-stent restenosis. *J Invasive Cardiol* 2005; 17: 369–370.

31. Matsumoto D., Shite J., Shinke T., et al. Neointimal coverage of sirolimus-eluting stents at 6-month follow-up: evaluated by optical coherence tomography. *Eur Heart* J 2007; 28: 961–967.

32. Farooq M.U., Khasnis A., Majid A., Kassab M.Y. The role of optical coherence tomography in vascular medicine. *Vascular Medicine* 2009; 14: 63–71.

33. Kubo T., Imanishi T., Takarada S., Kuroi A., Ueno S., Yamano T., et al. Assessment of culprit lesion morphology in acute myocardial infarction: ability of optical coherence tomography compared with intravascular ultrasound and coronary angioscopy. *J Am Coll Cardiol* 2007 Sep 4; 50(10): 933–939.

34. Kume T., Akasaka T., Kawamoto T., Okura H., Watanabe N., Toyota E., et al. Measurement of the thickness of the fibrous cap by optical coherence tomography. *Am Heart J* 2006; 152(755): 751–754.

35. Sawada T., Shite J., Garcia-Garcia H.M., Shinke T., Watanabe S., Otake H., et al. Feasibility of combined use of intravascular ultrasound radiofrequency data analysis and optical coherence tomography for detecting thin-cap fibroatheroma. *European Heart Journal* 2008 April 7; 29: 1136–1146.

36. Kubo T., Imanishi T., Takarada S., Kuroi A., Ueno S., Yamano T., et al. Implication of plaque color classification for assessing plaque vulnerability: a coronary angioscopy and optical coherence tomography investigation. *JACC Cardiovasc Interv* 2008; 1: 74–80.

37. Kashiwagi M., Tanaka A., Kitabata H., Tsujioka H., Kataiwa H., Komukai K., et al. Feasibility of noninvasive assessment of thin-cap fibroatheroma by multidetector computed tomography. *JACC Cardiovasc Imaging* 2009; 2: 1412–1419.

38. Fujii K., Masutani M., Okumura T., Kawasaki D., Akagami T., Ezumi A., et al. Frequency and predictor of coronary thin-cap fibroatheroma in patients with acute myocardial infarction and stable angina pectoris a 3-vessel optical coherence tomography study. *J Am Coll Cardiol* 2008; 52: 787–788.

39. Greenland P., Bonow R.O., Brundage B.H., Budoff M.J., Eisenberg M.J., Grundy S.M., et al. ACCF/AHA 2007 clinical expert consensus document on coronary artery calcium scoring by computed tomography in global cardiovascular risk assessment and in evaluation of patients with chest pain: a report of the american college of cardiology foundation clinical expert consensus task force (ACCF/AHA writing committee to update the 2000 expert consensus document on electron beam computed tomography) developed in collaboration with the society of atherosclerosis imaging and prevention and the society of cardiovascular computed tomography. *J Am Coll Cardiol* 2007; 49(3): 378–402.

40. Mintz G.S., Popma J., Pichard A.D., Kent K.M., Satler L.F., Chuang Y.C., et al. Patterns of calcification in coronary artery disease. A statistical analysis of intravascular ultrasound and coronary angiography in 1155 lesions. *Circulation* 1995; 91: 1959–1965.

41. Wexler L., Brundage B., Crouse J., Detrano R., Fuster V., Maddahi J., et al. Coronary artery calcification: pathophysiology, epidemiology, imaging methods, and clinical implications. A statement for health professionals from the American heart association. Writing group. *Circulation* 1996; 94: 1175–1192.

42. Agatston A.S., Janowitz W.R., Hildner F.J., Zusmer N.R., Viamonte M.J., Detrano R. Quantification of coronary artery calcium using ultrafast computed tomography. *J Am Coll Cardiol* 1990; 15: 827–832.

43. Carr J.J., Nelson J.C., Wong N.D., McNitt-Gray M., Arad Y., Jacobs J., et al. Calcified coronary artery plaque measurement with cardiac ct in population-based studies: standardized protocol of multi-ethnic study of atherosclerosis (mesa) and coronary artery risk development in young adults (cardia) study. *Radiology* 2005; 234: 35–43.

44. Callister T.Q., Cooil B., Raya S.P., Lippolis N.J., Russo D.J., Raggi P. Coronary artery disease: improved reproducibility of calcium scoring with an electron-beam ct volumetric method. *Radiology* 1998; 208: 807–814.

45. Mintz G.S., Pichard A.D., Kovach J.A., Kent K.M., Satler L.F., Javier S.P., et al. Impact of preintervention intravascular ultrasound imaging on transcatheter treatment strategies in coronary artery disease. *Am J Cardiol* 1994; 73: 423–430.

46. Moussa I., Di Mario C., Moses J., Reimers B., Di Francesco L., Martini G., et al. Coronary stenting after rotational atherectomy in calcified and complex lesions. Angiographic and clinical follow-up results. *Circulation* 1997; 96: 128–136.

47. Kubo T., Xu C., Wang Z., van Ditzhuijzen N.S., Bezerra H.G. Plaque and thrombus evaluation by optical coherence tomography. *Int J Cardiovasc Imaging* 2011; 27(2): 289–298.

48. Wang Z., Kyono H., Bezerra H.G., Wang H., Gargesha M., Alraies C., et al. Semi-automatic segmentation and quantification of calcified plaques in intracoronary optical coherence tomography images. *J Biomed Opt* 2010; 15: 061711.

49. Lusis A.J. Atherosclerosis. *Nature* 2000; 407: 233–241.

50. Moreno P.R., Falk E., Palacios I.F., Newell J.B., Fuster V., Fallon J.T. Macrophage infiltration in acute coronary syndromes. Implications for plaque rupture. *Circulation* 1994; 90: 775–778.

51. MacNeill B.D., Bouma B.E., Yabushita H., Jang I.K., Tearney G.J. Intravascular optical coherence tomography: cellular imaging. *J Nucl Cardiol* 2005; 12: 460–465.

52. MacNeill B.D., Jang I.K., Bouma B.E., Iftimia N., Takano M., Yabushita H., et al. Focal and multi-focal plaque distributions in patients with macrophage acute and stable presentations of coronary artery disease. *Journal of the American College of Cardiology* 2004 Sep 1; 44(5): 972–979.

53. Drexler W., Morgner U., Kartner F.X., Pitris C., Boppart S.A., Li X.D., et al. In vivo ultrahighresolution optical coherence tomography. *Opt Lett* 1999; 24: 1221–1223.

54. Kume T., Akasaka T., Kawamoto T., Ogasawara Y., Watanabe N., Toyota E., et al. Assessment of coronary arterial thrombus by optical coherence tomography. *Am J Cardiol* 2006 Jun 15; 97(12): 1713–1717.

55. Mehanna E.A., Attizzani G.F., Kyono H., Hake M., Bezerra H.G. Assessment of coronary stent by optical coherence tomography, methodology and definitions. *Int J Cardiovasc Imaging* 2011; 27(2): 259–269.

56. Yao Z.H., Matsubara T., Inada T., Suzuki Y., Suzuki T. Neointimal coverage of sirolimus-eluting stents 6 months and 12 months after implantation: evaluation by optical coherence tomography. *Chin Med J* 2008; 121: 503–507.

57. Gonzalo N., Garcia-Garcia H.M., Serruys P.W., Commissaris K.H., Bezerra H., Gobbens P., Costa M., Regar E. Reproducibility of quantitative optical coherence tomography for stent analysis. *EuroIntervention* 2009; 5(2): 224–232.

58. Rosenthal N., Guagliumi G., Sirbu V. Comparison of intravascular ultrasound and optical coherence tomography for the evaluation of stent segment malapposition. *J Am Coll Cardiol* 2009; 53 (A1–A99 (supplement)).

59. Suzuki Y., Ikeno F., Koizumi T., Tio F., Yeung A.C., Yock P.G., Fitzgerald P.J., Fearon W.F. In vivo comparison between optical coherence tomography and intravascular ultrasound for detecting small degrees of in-stent neointima after stent implantation. *JACC Cardiovasc Interv* 2008; 1(2): 168–173.

60. Guagliumi G., Musumeci G., Sirbu V., Bezerra H.G., et al. Optical coherence tomography assessment of in vivo vascular response after implantation of overlapping bare-metal and drug-eluting stents. *JACC Cardiovasc Interv* 2010; 3(5): 531–539.

61. Guagliumi G., Sirbu V., Bezerra H., Biondi-Zoccai G., Fiocca L., et al. Strut coverage and vessel wall response to zotarolimus-eluting

and bare-metal stents implanted in patients with ST-segment elevation myocardial infarction: the OCTAMI (Optical coherence tomography in acute myocardial infarction) study. *JACC Cardiovasc Interv* 2010; 3(6): 680–687.

62. Guagliumi G., Sirbu V., Musumeci G., Bezerra H.G., Aprile A., Kyono H., et al. Strut coverage and vessel wall response to a new-generation paclitaxel-eluting stent with an ultrathin biodegradable abluminal polymer: optical coherence tomography drug-eluting stent investigation (OCTDESI). *Circ Cardiovasc Interv* 2010; 3(4): 367–375.

63. Guagliumi G., Sirbu V. Optical coherence tomography: high resolution intravascular imaging to evaluate vascular healing after coronary stenting. *Catheter Cardiovasc Interv* 2008; 72(2): 237–247.

64. Takarada S., Imanishi T., Liu Y., Ikejima H., Tsujioka H., Kuroi A., Ishibashi K., et al. Advantage of next-generation frequency-domain optical coherence tomography compared with conventional time-domain system in the assessment of coronary lesion. *Catheter Cardiovasc Interv* 2010; 75(2): 202–206.

65. Capodanno D., Prati F., Pawlowsky T., Cera M., La M.A., Albertucci M., et al. Comparison of optical coherence tomography and intravascular ultrasound for the assessment of in-stent tissue coverage after stent implantation. *EuroIntervention* 2009; 5(5): 538–543.

66. Onuma Y., Serruys P.W., Perkins L.E., Okamura T., Gonzalo N., Garcia-Garcia H.M., et al. Intracoronary optical coherence tomography and histology at 1 month and 2, 3, and 4 years after implantation of everolimus-eluting bioresorbable vascular scaffolds in a porcine coronary artery model: an attempt to decipher the human optical coherence tomography images in the ABSORB trial. *Circulation* 2010; 122(22): 2288–2300.

67. Murata A., Wallace-Bradley D., Tellez A., Alviar C., Aboodi M., Sheehy A., Coleman L., Perkins L., et al. Accuracy of optical coherence tomography in the evaluation of neointimal coverage after stent implantation. *JACC Cardiovasc Imaging* 2010; 3(1): 76–84.

68. Bezerra H.G., Guagliumi G., Valescchi O., Lortkipanidze N., Rosenthal N., Tahara S., Kyono H., et al. Unraveling the lack of Neointimal hyperplasia detected by intravascular ultrasound using optical coherence tomography: lack of spatial resolution or a true biological effect? *J Am Coll Cardiol* 2009; 10(Suppl A): 90A.

69. Finn A.V., Joner M., Nakazawa G., et al. Pathological correlates of late drugeluting stent thrombosis: strut coverage as a marker of endothelialization. *Circulation* 2007; 115(18): 2435–2441.

70. Cook S., Wenaweser P., Togni M., Billinger M., et al. Incomplete stent apposition and very late stent thrombosis after drug-eluting stent implantation. *Circulation* 2007; 115(18): 2426–2434.

71. Caldera A.E., Cruz-Gonzalez I., Bezerra H.G., Cury R.C., Palacios I.F., Cockrill B.A., Inglessis-Azuaje I. Endovascular therapy for left main compression syndrome. Case report and literature review. *Chest* 2009; 135(6): 1648–1650.

72. Ishigami K., Uemura S., Morikawa Y., Soeda T., Okayama S., Nishida T., Takemoto Y., et al. Long-term follow-up of neointimal coverage of sirolimus-eluting stents: evaluation with optical coherence tomography. *Circ J* 2009; 73(12): 2300–2307.

73. Miyoshi N., Shite J., Shinke T., Otake H., Tanino Y., Ogasawara D., Sawada T., Kawamori H., et al. Comparison by optical coherence tomography of paclitaxel-eluting stents with sirolimuseluting stents implanted in one coronary artery in one procedure — 6-month follow-up. *Circ J* 2010; 74(5): 903–908.

74. Suzuki N., Guagliumi G., Bezerra H.G., Sirbu V., Rosenthal N., Musumeci G., Aprile A., Wang H., et al. The impact of an eccentric intravascular image wire during coronary optical coherence tomography imaging. *EuroIntervention* 2011; 6(8): 963–969.

75. Prati F., Regar E., Mintz G.S., Arbustini A., Di Mario C., Jang I.K., Akasaka T., Costa M., et al. Expert review document on methodology, terminology, and clinical applications of optical coherence tomography: physical principles, methodology of image acquisition, and clinical application for assessment of coronary arteries and atherosclerosis. *Eur Heart J* 2010; 31(4): 401–415.

76. Regar E., Serruys P.W., Van Leeuwen T.Ge. *Optical coherence tomography in cardiovascular research*. London: Informa Healthcare; 2007.

77. Prati F., Jenkins M.W., Giorgio A.D., Rollins A.M. Intracoronary optical coherence tomography, basic theory and image acquisition techniques. *Int Journal of Cardiac Imaging* 2011 Feb; 27(2): 251–258.

78. Giattina S.D., Courtney B.K., Herz P.R., Harman M., Shortkroff S., Stamper D.L., et al. Assessment of coronary plaque collagen with polarization sensitive optical coherence tomography (PS-OCT). *Int J Cardiol* 2006 Mar 8; 107(3): 400–409.

79. Nadkami S.K., Pierce M.C., Park B.H., de Boer J.F., Whittaker P., Bouma B.E., et al. Measurement of collagen and smooth muscle cell content in atherosclerotic plaques using polarization-sensitive optical coherence tomography. *Journal of the American College of Cardiology* 2007; 49(13): 1474–1481.

80. Chen Z., Milner T.E., Srinivas S., Wang X., Malekafzali A., Gemert M.J.C., Nelson J.S. Noninvasive imaging of in vivo blood flow velocity using optical Doppler tomography. *Opt Lett* 1997; 22(14): 1119–1121.

81. Drexler W., Fujimoto J. *Optical Coherence Tomography*. Berlin, Heidelberg; 2008.

82. Yazdanfar S., Kulkarni M., Izatt J. High resolution imaging of in vivo cardiac dynamics using color Doppler optical coherence tomography. *Opt Express* 1997; 1(13): 424–431.

83. Levitz D., Thrane L., Frosz M., Andersen P., Andersen C., Andersson-Engels S., et al. Determination of optical scattering properties of highly-scattering media in optical coherence tomography images. *Opt Express* 2004; 12: 249–259.

84. van der Meer F.J., Faber D.J., Baraznji Sassoon D.M., Aalders M.C., Pasterkamp G., van Leeuwen T.G. Localized measurement of optical attenuation coefficients of atherosclerotic plaque constituents by quantitative optical coherence tomography. IEEE Transactions on Medical Imaging 2005 Oct; 24(10): 1369–1376.

85. Xu C., Schmitt J.M., Carlier S.G., Virmani R. Characterization of atherosclerosis plaques by measuring both backscattering and attenuation coefficients in optical coherence tomography. *J Biomed Opt* 2008; 13: 034003.

86. van Soest G., Goderie T., Regar E., Koljenovic S., van Leenders G.L., Gonzalo N., et al. Atherosclerotic tissue characterization in vivo by optical coherence tomography attenuation imaging. *J Biomed Opt* 2010; 15: 011105.

87. Tearney G.J., Waxman S., Shishkov M., Vakoc B.J., Suter M.J., Freilich M.I., et al. Three-dimensional coronary artery microscopy by intracoronary optical frequency domain imaging: first-in-man experience. *JACC Cardiovasc Imaging* 2008; 1: 752–761.

88. Izatt J.A., Kulkarni M.D., Yazdanfar S., Barton J.K., Welch A.J. In vivo bidirectional color doppler flow imaging of picoliter blood volumes using optical coherence tomography. *Opt Lett* 1997; 22: 1439–1441.

89. Wang X.J., Milner T.E., Nelson J.S. Characterization of fluid flow velocity by optical Doppler tomography. Opt Lett 1995; 20: 1337–1339.

90. de Boer J.F., Milner T.E., van Gemert M.J.C., Nelson J.S. Two dimensional birefringence imaging in biological tissue by polarization-sensitive optical coherence tomography. *Opt Lett* 1997; 22: 934–936.

91. Everett M.J., Schoenenberger K., Colston J.B.W., Da Silva L.B. Birefringence characterization of biological tissue by use of optical coherence tomography. *Opt Lett* 1998; 23: 228–230.

92. Hee M.R., Huang D., Swanson E.A., Fujimoto J.G. Polarizationsensitive low-coherence reflectometer for birefringence characterization and ranging. *J Opt Soc Am B* 1992; 9: 903–908.

93. Applegate B.E., Izatt J.A. Molecular imaging of endogenous and exogenous chromophores using ground state recovery pump-probe optical coherence tomography. *Opt Exp* 2006; 14: 9142–9155.

94. Xu C., Ye J., Marks D.L., Boppart S.A. Near-infrared dyes as contrast-enhancing agents for spectroscopic optical coherence tomography. *Opt Lett* 2004; 29: 1647–1649.

95. Yang C., Choma M.A., Lamb L.E., Simon J.D., Izatt J.A. Protein-based molecular contrast optical coherence tomography with phytochrome as the contrast agent. *Opt Lett* 2004; 29: 1396–1398.

96. An L., Wang R.K. In vivo volumetric imaging of vascular

perfusion within human retina and choroids with optical micro-angiography. *Opt Exp* 2008; 16: 11438–11452.

97. Park B.H., Pierce M.C., Cense B., Yun S.H., Mujat M., Tearney G.J., et al. Real-time fiber-based multi-functional spectral-domain optical coherence tomography at 1.3 mm. *Opt Exp* 2005; 13: 3931–3944.

98. Szkulmowska A., Szkulmowski M., Kowalczyk A., Wojtkowski M. Phase-resolved Doppler optical coherence tomography-limitations and improvements. *Opt Lett* 2008; 33: 1425–1427.

99. Vakoc B.J., Yun S.H., de Boer J.F., Tearney G.J., Bouma B.E. Phaseresolved optical frequency domain imaging. *Opt Exp* 2005; 13: 5483–5493.

100. Oh W.Y., Vakoc B.J., Yun S.H., Tearney G.J., Bouma B.E. Single-detector polarization-sensitive optical frequency domain imaging using high-speed intra a-line polarization modulation. *Opt Lett* 2008; 33: 1330–1332.

101. Yamanari M., Makita S., Madjarova V.D., Yatagai T., Yasuno Y. Fiber-based polarization-sensitive fourier domain optical coherence tomography using b-scan-oriented polarization modulation method. *Opt Exp* 2006; 14: 6502–6515.